Electronic Supplementary Material (ESI) for Journal of Materials Chemistry C.

Supporting Information

Explicating the Irreversible Electric-Field-Assisted Ferroelectric Phase Transition in the Otherwise Antiferroelectric Sodium Niobate for Energy Storage Systems

Kwangrae Kim,* Woohyun Hwang,* Ji-Hwan Lee,† and Aloysius Soon‡

Department of Materials Science & Engineering,

Yonsei University, Seoul 03722, Republic of Korea

S1. PHASE TRANSITIONS DRIVEN BY SOFT PHONON MODES

Harmonic phonon dispersion calculations have been carried out to determine the phonon eigendisplacement vectors with a set of atomic displacements while considering the related symmetries of the crystal structures containing the displaced atoms. Note that the imaginary frequencies in the phonon dispersion curve are indicative of soft phonon modes (in the first Brillouin zone) that drives the specific phase transition, namely at the Γ (0,0,0), X $(\frac{1}{2}, 0, 0)$, M $(\frac{1}{2}, \frac{1}{2}, 0)$, and R $(\frac{1}{2}, \frac{1}{2}, \frac{1}{2})$ **q**-points. At the Γ **q**-point, only one soft phonon mode (Γ_4^-) appears at $5.103i$ THz with a three-fold degeneracy. At the M **q**-point, there are two non-degenerate soft phonon modes shown at $3.516i$ THz and $1.655i$ THz, which correspond to the M_2^+ and M_2^- mode, respectively. At the R **q**-point, there is one three-fold degenerated soft phonon mode (R_5^-) at $3.838i$ THz, while at the X **q**-point, one soft phonon mode (X_5^+) is located at $2.931i$ THz with a two-fold degeneracy.

* Contributed equally to this work

† jkwnlee88@yonsei.ac.kr

‡ aloysius.soon@yonsei.ac.kr

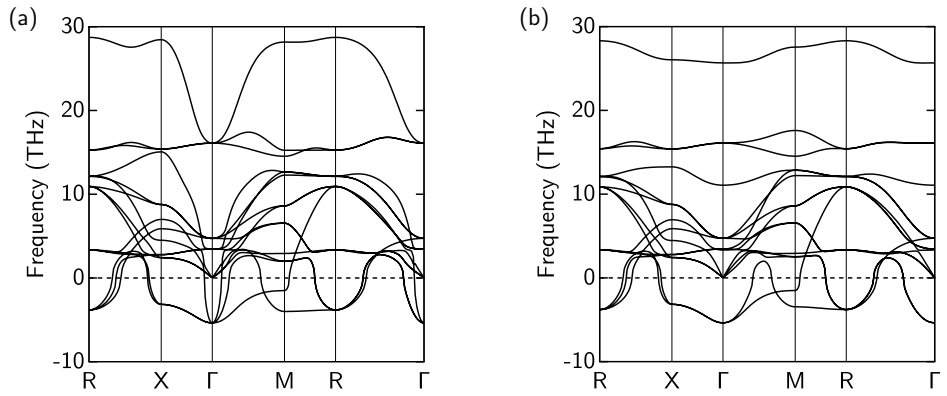

FIGURE S1. DFT-PBEsol phonon band structure for the aristotype cubic $NaNbO_3$ (U phase; $Pm\bar{3}m$) – (a) without and (b) with the non-analytical-term correction (NAC) [1] applied to dynamical matrix, respectively.

TABLE S1. DFT-PBEsol (imaginary) phonon frequencies (in THz) and their degeneracies, irreducible representations (IR with modes labelled), directions of the order parameter, crystal symmetries of the relaxed structure, the number of atoms per cell, and their calculated relative energies (in meV/formula-unit) with respect to the cubic $Pm\bar{3}m$ (U) $NaNbO_3$ phase.

ω (THz)	Degeneracy	Mode	Direction	Symmetry	No. of atoms	ΔE (meV/f.u.)
$5.103i$	3	Γ_4^-	$(a,0,0)$	$P4mm$	5	-30.5
			$(a,a,0)$	$Amm2$	10	-32.5
			(a,a,a)	$R3m$	15	-31.8
$3.838i$	3	R_5^-	$(a,0,0)$	$I4/mcm$	20	-70.8
			$(a,a,0)$	$Imma$	20	-81.9
			(a,a,a)	$R\bar{3}c$	30	-79.2
$3.516i$	1	M_2^+	$(a;0;0)$	$P4/mbm$	10	-66.2
$2.931i$	2	X_5^+	$(0,a;0,0;0,0)$	$Pmma$	10	-4.0
			$(a,a;0,0;0,0)$	$Cmcm$	20	-4.1
$1.655i$	1	M_2^-	$(a;0;0)$	$P4/nmm$	10	-2.8

TABLE S2. DFT-PBEsol optimized crystal phases of $NaNbO_3$ known from experiments: Crystal symmetries of the relaxed structure, irreducible representations (IR with modes labelled), directions of the order parameter, basis vectors, the number of atoms per cell, and their calculated relative energies (in meV/formula-unit) with respect to the cubic $Pm\bar{3}m$ (U) $NaNbO_3$ phase.

Symmetry	Mode(s)	Direction(s)	Basis vector	No. of atoms	ΔE (meV/f.u.)
$Pm\bar{3}m\,(U)$	-	-	$(1,1,1)$	5	0
$P4mm$	Γ_4^-	$(a,0,0)$	$(1,1,1)$	5	-31.8
$R3m$	Γ_4^-	(a,a,a)	$(\sqrt{2},\sqrt{2},\sqrt{3})$	15	-32.8
$Amm2$	Γ_4^-	$(a,a,0)$	$(\sqrt{2},\sqrt{2},1)$	10	-33.7
$P4/mbm\,(T_2)$	M_2^+	$(a;0;0)$	$(\sqrt{2},\sqrt{2},1)$	10	-66.2
$I4/mcm$	T_2	$(a,0;0,0;0,0)$	$(\sqrt{2},\sqrt{2},4)$	40	-68.5
$P4/mbm$	M_2^+, T_2	$(a,0,0)$, $(a,0;0,0;0,0)$	$(\sqrt{2},\sqrt{2},3)$	30	-69.3
$I4/mcm$	R_5^-	$(a,0,0)$	$(\sqrt{2},\sqrt{2},4)$	20	-70.8
$R\bar{3}c$	R_5^-	(a,a,a)	$(\sqrt{2},\sqrt{2},2\sqrt{3})$	30	-79.2
$Imma$	R_5^-	$(0,a,-a)$	$(\sqrt{2},2,\sqrt{2})$	20	-81.9
$Cmcm\,(T_1)$	M_2^+, R_5^-	$(a;0;0)$, $(0,0,a)$	$(2,2,2)$	40	-84.8
$Pmmn\,(S)$	M_2^+, R_5^-	$(a;b;0)$, $(0,0,a)$	$(2,2,4)$	80	-87.3
$Pnma$	M_2^+, R_5^-	$(a;0;0)$, $(0,a,a)$	$(\sqrt{2},2,\sqrt{2})$	20	-92.9
$Pmmn\,(R)$	M_2^+, R_5^-, T_2	$(0;a;b)$, $(a,0,0)$, $(0,0;a,0;0,0)$	$(2,6,2)$	120	-101.4
$Pnma\,(R)$	M_2^+, R_5^-, T_2	$(0;0;a)$, $(0,a,0)$, $(0,a,0,0,0,0)$	$(2,2,6)$	120	-102.0
$Pmc2_1\,(Q)$	M_2^+, R_5^-, Γ_4^-	$(a;0;0)$, $(0,a,a)$, $(a,a,0)$	$(2,\sqrt{2},\sqrt{2})$	20	-109.8
$Pbcm\,(P)$	R_5^-, T_2	$(0,a,a)$, $(a,0;0,0;0,0)$	$(\sqrt{2},\sqrt{2},4)$	40	-110.0
$R3c\,(N)$	R_5^-, Γ_4^-	(a,a,a), (a,a,a)	$(\sqrt{2},\sqrt{2},2\sqrt{3})$	30	-112.0

S2. RATIONALIZATION OF POTENTIAL ENERGY SURFACES (PES) BY SYMMETRY-ADAPTED MODE ANALYSIS

Potential energy surfaces (PES) are graphed based on the symmetry-adapted modes with diverse and feasible combinations of any two major modes with considering both *competitive* and *cooperative* relations between the modes in lowering the overall energy of the crystal during a phase transition. The phonon mode amplitudes, $\mathcal{Q}$ (in Å) of the R_5^-, Δ_5, and T_2 modes are normalized to match the $\mathcal{Q}$ values in the P phase while the corresponding $\mathcal{Q}$ values for Γ_4^- and M_2^+ are also normalized for the Q phase in a similar fashion. To paint a simple picture of this *competitive* or/and *cooperative* relationship between the major phonon modes, the PES for different sets of combinatorial modes can be found in Figures S2 and S3 (*competitive* relations) and Figures S4 and S5 (*cooperative* relations).

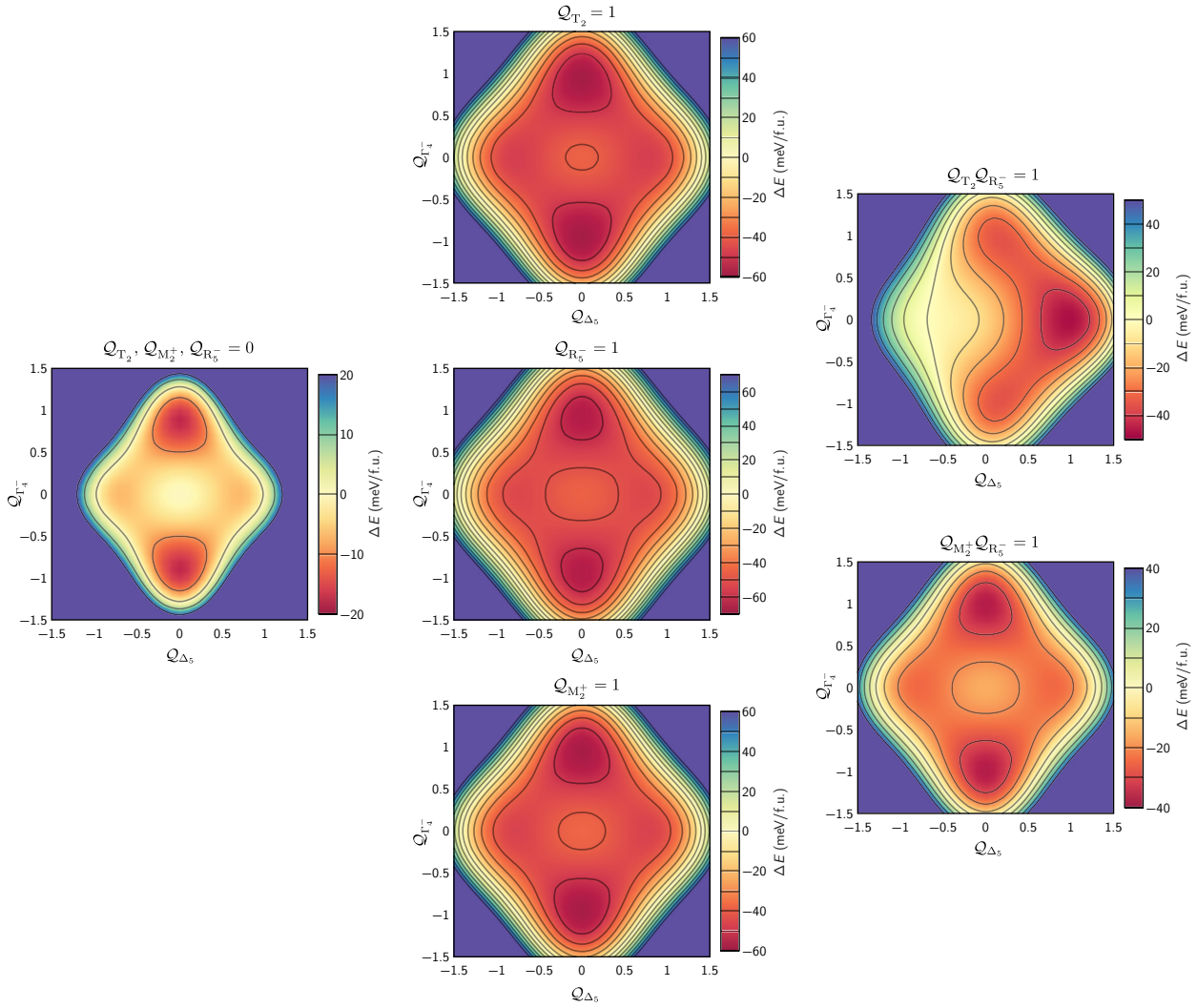

FIGURE S2. (Left column) Potential energy surface (PES) constructed via the anti-polar Δ_5 mode versus the polar Γ_4^- mode, where all other modes are not included, i.e., $\mathcal{Q}_{T_2}, \mathcal{Q}_{M_2^+}$, and $\mathcal{Q}_{R_5^-} = 0$. (Middle column; From top to bottom) PES now constructed by including only one other mode: $\mathcal{Q}_{T_2} = 1$, $\mathcal{Q}_{R_5^-} = 1$, and $\mathcal{Q}_{M_2^+} = 1$ (in addition to Δ_5 and Γ_4^-), respectively. (Right column; From top to bottom) PES now includes the additional consideration of two other modes (other than Δ_5 and Γ_4^-): $\mathcal{Q}_{T_2}\mathcal{Q}_{R_5^-} = 1$ and $\mathcal{Q}_{M_2^+}\mathcal{Q}_{R_5^-} = 1$, respectively.

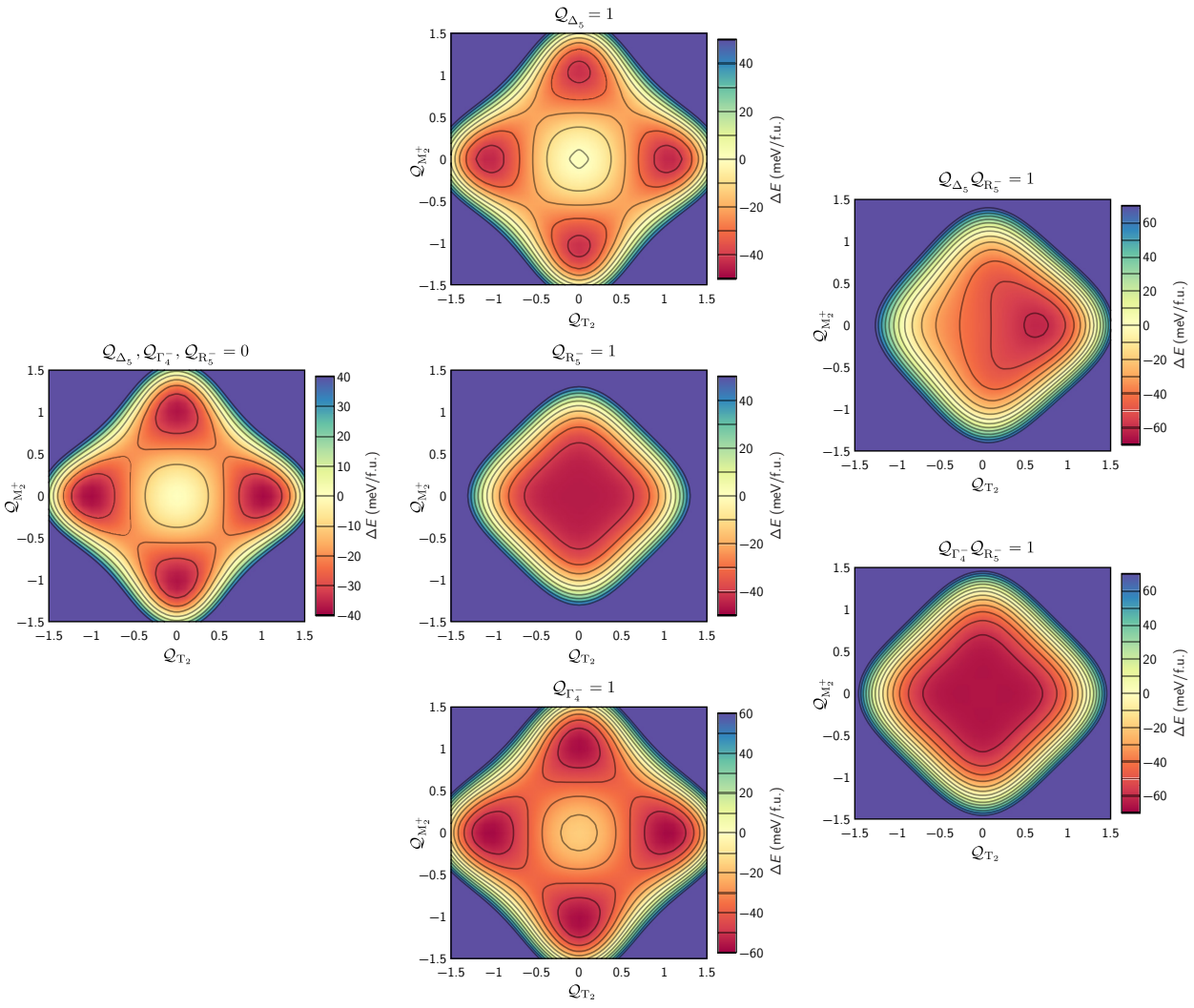

FIGURE S3. (Left column) Potential energy surface (PES) constructed via the in-phase/out-of-phase ($a^0a^0a^+/a^0a^0a^-$) rotation T_2 mode versus the in-phase ($a^0a^0a^+$) rotation M_2^+ mode, where all other modes are not included, i.e., $\mathcal{Q}_{\Delta_5}, \mathcal{Q}_{\Gamma_4^-}$, and $\mathcal{Q}_{R_5^-} = 0$. (Middle column; From top to bottom) PES now constructed by including only one other mode: $\mathcal{Q}_{\Delta_5} = 1$, $\mathcal{Q}_{R_5^-} = 1$, and $\mathcal{Q}_{\Gamma_4^-} = 1$ (in addition to T_2 and M_2^+), respectively. (Right column; From top to bottom) PES now includes the additional consideration of two other modes (other than T_2 and M_2^+): $\mathcal{Q}_{\Delta_5}\mathcal{Q}_{R_5^-} = 1$ and $\mathcal{Q}_{\Gamma_4^-}\mathcal{Q}_{R_5^-} = 1$, respectively.

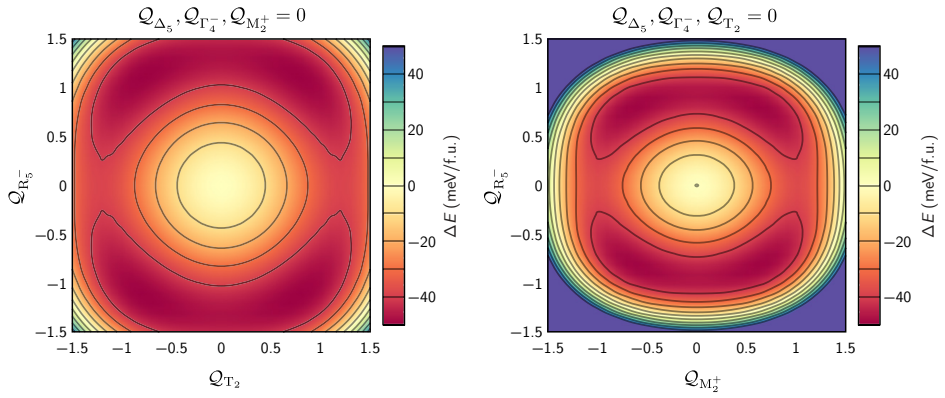

FIGURE S4. (Left) Potential energy surface (PES) constructed via the in-phase/out-of-phase ($a^0a^0a^+/a^0a^0a^-$) rotation T_2 mode versus the out-of-phase ($a^-a^-a^0$) tilting R_5^- mode, where all other modes are not included, i.e., $\mathcal{Q}_{\Delta_5}, \mathcal{Q}_{\Gamma_4^-}$, and $\mathcal{Q}_{M_2^+} = 0$. (Right) PES constructed via the in-phase ($a^0a^0a^+$) rotation M_2^+ mode versus the out-of-phase tilting R_5^- mode, where all other modes are not included, i.e., $\mathcal{Q}_{\Delta_5}, \mathcal{Q}_{\Gamma_4^-}$, and $\mathcal{Q}_{T_2} = 0$.

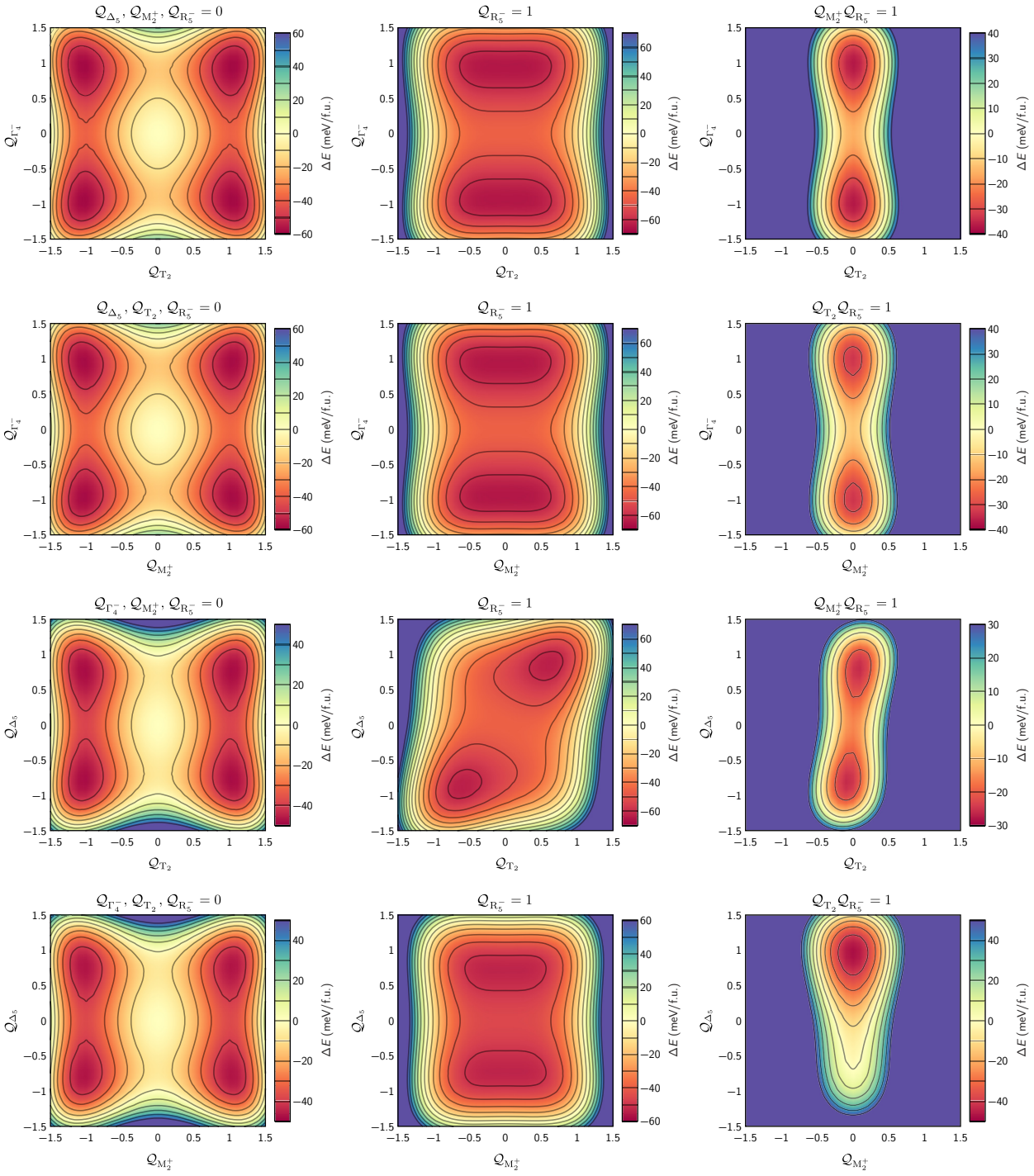

FIGURE S5. Similar to Figures S2 to S4, moving to left to right for each row, the interplay of two selected modes are chosen, firstly with all other modes set to zero, and with the inclusion of one more specific mode, and then the inclusion of two more modes.

[1] X. Gonze. Adiabatic Density-Functional Perturbation Theory. *Phys. Rev. A* **1995**, *52*, 1096.